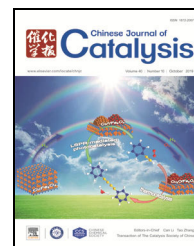


available at www.sciencedirect.comjournal homepage: www.elsevier.com/locate/chnjc

Communication

Aliphatic amines modified CoO nanoparticles for catalytic oxidation of aromatic hydrocarbon with molecular oxygen

Meng Liu ^{a,b}, Song Shi ^{a,#}, Li Zhao ^{a,b}, Chen Chen ^{a,c}, Jin Gao ^a, Jie Xu ^{a,*}

^a State Key Laboratory of Catalysis, Dalian Institute of Chemical Physics, Chinese Academy of Sciences, Dalian National Laboratory for Clean Energy, Dalian 116023, Liaoning, China

^b University of Chinese Academy of Sciences, Beijing 100049, China

^c School of Materials Science & Chemical Engineering, Ningbo University, Ningbo 315211, Zhejiang, China

ARTICLE INFO

Article history:

Received 28 June 2019

Accepted 19 July 2019

Published 5 October 2019

Keywords:

Hydrocarbon oxidation

Hydrophobic modification

Amines coating

Cobalt oxide

Surface modification

ABSTRACT

The surface modification of metal oxides using organic modifiers is a potential strategy for enhancing their catalytic performances. In this study, a hydrophobic surface amine-modified CoO catalyst with a water contact angle of 143° was fabricated. The catalyst was characterized by XRD, TGA, FT-IR, HR-TEM, and XPS. The results showed that the fabricated catalyst performed better than the hydrophilic commercial CoO nanoparticle in the process of aromatic hydrocarbon oxidation. After the amines modification, commercial CoO also became hydrophobic and improved conversion of ethylbenzene was achieved. The surface modification of CoO with amines induced the hydrophobicity property, which could serve as a reference for the design of other hydrophobic catalysts.

© 2019, Dalian Institute of Chemical Physics, Chinese Academy of Sciences.

Published by Elsevier B.V. All rights reserved.

The selective oxidation of hydrocarbons to oxygen-containing compounds with dioxygen is an important process in both academic research and industrial production [1–3]. The difficulties in this process lie in the activation of the inert C–H bond and the selectivity toward the alcohols and ketones, which are more active than the hydrocarbons [4,5]. Metal oxides nanoparticles are efficient catalysts for hydrocarbon oxidation. Several metal oxides have been developed to improve the efficiency of this process, including Mn₃O₄ [6], CoO_x [7], and CuO_x [8,9]. Among these catalyst systems, CoO_x exhibited excellent performance, particularly the nano-sized particles. The porosity [10], particle size [11], and co-component [12] of CoO_x nanoparticles have been investigated. Many other factors that could enhance the reaction rate of a heterogeneous catalysis

reaction exist, such as the electronic state [13] and the micro-environment [14]. The surface hydrophobicity of the catalyst was advantageous to the hydrocarbon oxidation owing to the nature of the process [15–19]. The CoO_x nanoparticles exhibited hydrophilic properties toward the polar hydroxyl groups on the surface. In our previous report [15,17], silica served as the co-component, and a common strategy of organosilane modification was applied to make the surface hydrophobic. The direct hydrophobic modification of CoO_x nanoparticles, which acted as active sites, has rarely been studied. The direct modification of nanoparticles to have a hydrophobic surface is challenging.

Organic modification is an important strategy for modifying the surface of catalysts [20,21]. Several researchers have reported the application of the modification method to improve

* Corresponding author. Tel/Fax: +86-411-84379245; E-mail: xujie@dicp.ac.cn

Corresponding author. Tel/Fax: +86-411-84379277; E-mail: shisong@dicp.ac.cn

This work was supported by the National Natural Science Foundation of China (21790331, 21603218) and the Strategic Priority Research Program of Chinese Academy of Sciences (XDA21030400, XDB17020300).

DOI: S1872-2067(19)63413-3 | <http://www.sciencedirect.com/science/journal/18722067> | Chin. J. Catal., Vol. 40, No. 10, October 2019

the selectivity of certain reactions. In particular, when organic modifiers, including organophosphonic acids [22], carboxylates [23], and 2-cyanopyridine [24], were employed, metal oxides such as CeO₂, TiO₂, and MnO₂ were promoted to achieve enhanced reaction performance. Our team has previously reported the green modification of the MnO₂ surface with carboxylates to adjust the selectivity of the desired product [23]. However, little attention was paid to the modification of CoO_x with aliphatic amines for aromatic hydrocarbon oxidation.

Here, amine-modified CoO nanoparticles were synthesized through the solvothermal approach to decompose a cobalt-oleate complex in 2-octanol solvent and amines system. The amines, which acted as organic modifiers, were *in-situ* introduced to the CoO during the synthesis process; the CoO nanoparticle exhibited hydrophobic characteristics and showed good performance in the aromatic hydrocarbon oxidation process. Two similar CoO nanoparticles, surface-coated with butylamine (BA) and dodecylamine (DA), were obtained and were denoted as BA-CoO and DA-CoO, respectively.

The X-ray diffraction (XRD) patterns in Fig. 1 show the bulk phase of the as-synthesized nanoparticles. Both BA-CoO and DA-CoO display main peaks at the (111), (200), and (220) planes of cubic CoO with a rock salt structure as the commercial CoO, confirming that the nanoparticles were in the CoO phase. This was also confirmed by the high resolution transmission electron microscopy (HR-TEM) (Fig. 2(d)) results, which exhibited a *d*-spacing value of 0.25 nm corresponding to the CoO (111) plane. The peak intensity of DA-CoO was weaker than those of BA-CoO and commercial CoO, which was attributed to the smaller particle size of DA-CoO, in agreement with the TEM results shown in Fig. 2.

The morphology of the particle and distribution of the particle size could be directly observed through TEM characterization. As can be seen in Figs. 2(c) and 2(f), the DA-CoO nanoparticles have a nano-cubic morphology and an average size of ~25 nm (Fig. S1). Similarly, the BA-CoO nanoparticles exhibit a nano-cubic morphology, although the size distribution is broad (Fig. S2). This difference may be owing to the stronger basicity of butylamine compared to that of dodecylamine, which accelerated the decomposition of Co-oleate and resulted in the larg-

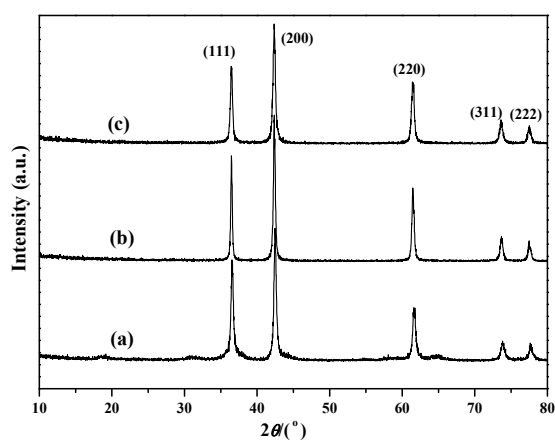


Fig. 1. XRD patterns of the commercial CoO (a), BA-CoO (b), and DA-CoO (c).

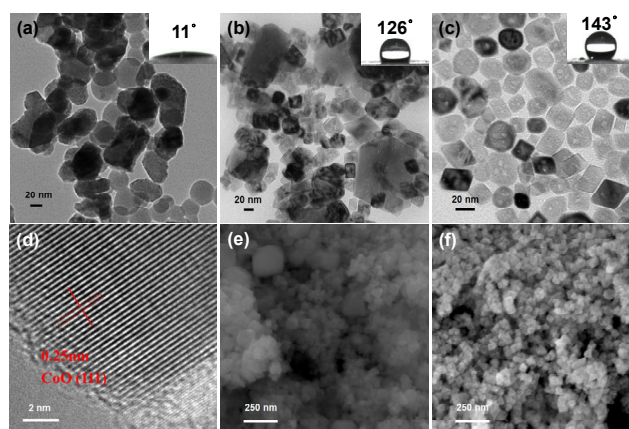


Fig. 2. TEM images of the commercial CoO (a), BA-CoO (b), and DA-CoO (c); (d) HRTEM of BA-CoO; SEM images of BA-CoO (e) and DA-CoO (f) (Insets are the images of sessile water droplets on the material film).

er size and broad distribution of BA-CoO. The commercial CoO has an average size of 49 nm, similar to that of BA-CoO (Fig. S3). This excludes the size effect on the reaction (*vide infra*). The hydrophobicity of the catalyst was characterized by water droplet contact angle measurements (WCA). The insets in Fig. 2 are the images of sessile water droplets on the material film. The commercial CoO is hydrophilic, and it has a WCA value below 20°. In contrast, BA-CoO has a WCA value of 126° and DA-CoO has a WCA value of 143°. This may be explained by the catalytic difference (*vide infra*). The difference in the WCA values also suggested that the surface of the as-synthesized CoO was coated by amines.

The existence of amines on the surface of the as-synthesized CoO was determined by Fourier transform infrared spectroscopy (FT-IR) and X-ray photoelectron spectroscopy (XPS). The nanoparticles were washed with hexane and ethanol until the FT-IR spectra remained unchanged to remove the organic compounds adsorbed (Figs. S4 and S5). The three samples presented broad absorption peaks at 3440 and 1630 cm⁻¹, which was attributed to the O–H stretching vibration and bending mode of the adsorbed water [25], respectively. The peaks at 2854 and 2926 cm⁻¹ in the FT-IR spectrum of DA-CoO are attributed to the C–H band vibration absorption. The peak at approximately 1040 cm⁻¹ could be ascribed to the stretching vibrations of the C–N bonds [26,27], and the peaks between 1300 and 1600 cm⁻¹ could be due to the –NH₂ group [28], which confirmed the existence of the amines on the surface (Fig. 3(c)). In contrast, no peaks attributed to the C–H band vibration absorption in the commercial CoO were observed. In comparison with that of DA-CoO, a weaker absorption peak appeared in the BA-CoO spectrum, which was attributed to the shorter length of butylamine compared to that of dodecylamine. Comparing BA-CoO with DA-CoO, the increase in the WCA could also be attributed to the longer length of dodecylamine (*vide supra*).

The XPS measurements confirmed that the amines existed on the surface of the nanoparticles based on the presence of N 1s peak (Figs. S7 and S8). The compositions of the samples are presented in Table S1. The N content in each sample is less than 1%, which is consistent with the TGA results (Fig. S9). The TGA

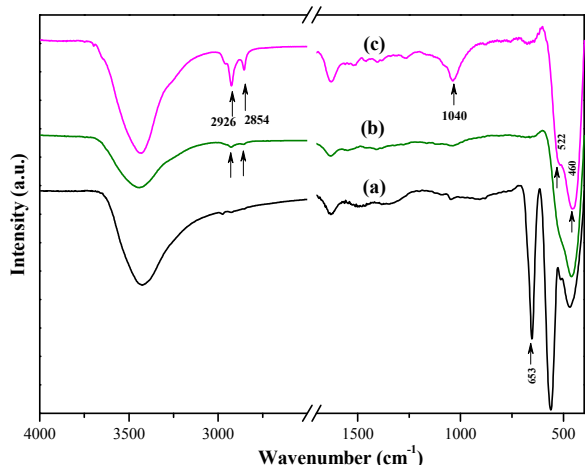


Fig. 3. FT-IR spectra of the commercial CoO (a), BA-CoO (b), and DA-CoO (c).

results showed a weight loss of 7% for DA-CoO and nearly no weight loss for the commercial CoO. For DA-CoO, there was an obvious weight loss at 410 °C, which was much higher than the boiling temperatures of 2-octanol (178 °C) and dodecylamine (259 °C). Furthermore, both the TGA results of 2-octanol and dodecylamine indicated a rapid weight loss at temperatures below 200 °C (Fig. S10). This confirmed the interaction between the amines and CoO nanoparticles to some extent. Although the XRD results confirmed that the nanoparticles are in the CoO phase, in the XPS measurement, Co(III) was detected. The Co 2*p* XPS spectra, as illustrated in Fig. 4, exhibited two main peaks at approximately 780.0 and 796.5 eV, assigned to Co 2*p*_{3/2} and Co 2*p*_{1/2}, respectively. Fitting the curves according to the characteristics of the cobalt oxides [29–31], the Co(III)/Co(II) ratio of the two samples are depicted in Table S1. Co(III) existed on the surface of the samples, which implied that a section of the surface of the CoO nanoparticle bore high valence Co(III). Using the FT-IR spectra to analyze the Co species, the peak located at 460 cm⁻¹ was attributed to the stretching vibration of the Co–O bond in CoO with a rock-salt structure, and the peak at 522 cm⁻¹ was attributed to the existence of

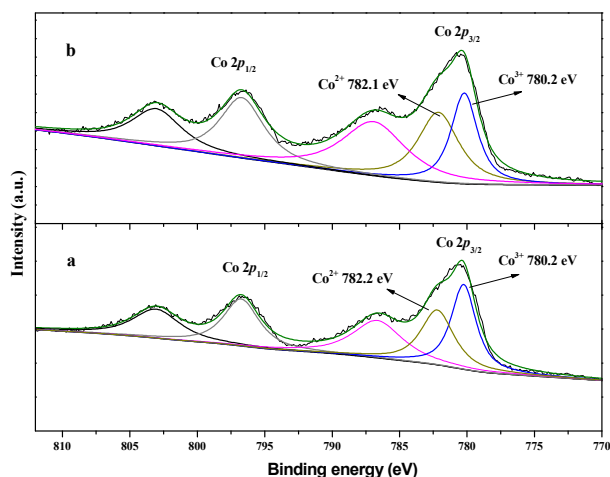


Fig. 4. Co 2*p* XPS spectra of DA-CoO (a) and BA-CoO (b).

small amounts of Co(III) [25]. The two bands observed at 653 and 561 cm⁻¹ were the characteristic vibrations of Co(II)–O and Co(III)–O bonds in Co₃O₄ [25,32], respectively, which implied the existence of Co(III) in the commercial CoO. The existence of Co(III) might favor the hydrocarbon oxidation [31], which can also be a factor for the enhancement of the catalytic performance.

The selective oxidation of ethylbenzene was conducted as the model reaction with the above materials as catalysts (Table 1). A remarkable difference was observed between the hydrophilic and hydrophobic catalysts. With the commercial hydrophilic CoO particles, the conversion was only 18% (Table 1, entry 3); in contrast, the hydrophobic DA-CoO exhibited a high conversion of 53% (Table 1, entry 2), which is almost twofold higher than that of commercial CoO particles. In addition, the selectivity of acetophenone increased from 69% to 78%. In the selective oxidation of hydrocarbons, alcohol is one of the primary oxidation products, which can be further oxidized to ketone. Higher selectivity towards ketones means that the hydrophobic DA-CoO has stronger oxidation ability. To investigate the vital factors for the catalytic differences between the commercial CoO and DA-CoO toward the selective oxidation of ethylbenzene, a few contrast experiments were conducted. First, a reaction was designed with the commercial CoO and additional DA as a catalyst to exclude the impact of dissociative DA. From the results, with a conversion of 17%, it can be deduced that the dissociative DA had no vital effect on the reaction (Table 1, entry 4). Subsequently, the hydrophilic and hydrophobic properties of CoO for the reaction were researched. When the commercial CoO was impregnated with 2-octanol and DA under stirring at room temperature for 5 h, it still had a hydrophilic surface with a WCA of 12° (Fig. S11), and the catalytic conversion was 20% (Table 1, entry 5). However, when the commercial CoO was impregnated with 2-octanol and DA at 250 °C for 5 h, the WCA reached 143°, which indicated the hydrophobic property of the amine treated commercial CoO (Fig. S12). With this hydrophobic catalyst, the conversion of ethylbenzene increased from 18% to 45%, and the selectivity of acetophenone increased from 69% to 81% (Table 1, entry 6). Besides, as shown in Fig. 5, the mass-specific activity for CoO was 92 mmol g_{cat}⁻¹ h⁻¹ after DA impregnation, which increased

Table 1

Selective oxidation of ethylbenzene with different catalysts.

Entry	Catalyst	Conversion (%)	Distribution of products (%)				
			1b	1c	1d	1e	1f
1	BA-CoO	50	16	79	4	1	0
2	DA-CoO	53	13	78	7	1	1
3	CoO	18	27	69	–	1	3
4 ^a	CoO	17	27	64	–	2	7
5 ^b	CoO	20	27	66	1	1	5
6 ^c	CoO	45	14	81	1	2	2

Reaction conditions: catalyst (20 mg), ethylbenzene (80 mmol), 1.0 MPa O₂, TBHP (80 mg) as initiator.

^a 1.6 mg DA was added; ^b the CoO was impregnated with DA at room temperature; ^c the CoO was impregnated with DA at 250 °C.

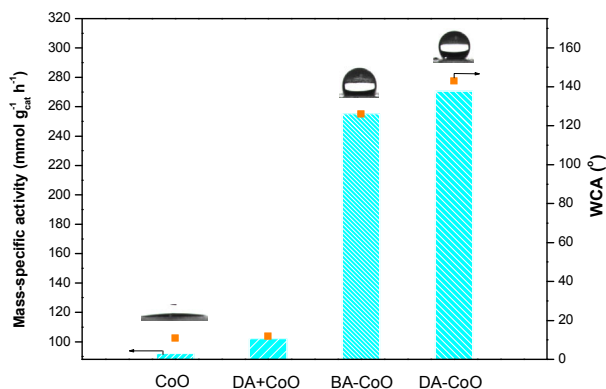


Fig. 5. Mass-specific activity (mmol g_{cat}⁻¹ h⁻¹) of CoO, and amines-modified CoO toward ethylbenzene oxidation with the variable WCA.

to 271 mmol g_{cat}⁻¹ h⁻¹ for DA-CoO, along with an increase in WCA from 11° to 143°. In summary, these contrasted results can verify that the hydrophobic surface is important for enhanced catalytic activity. Furthermore, the reusability of the DA-CoO was investigated by recycling experiments. The catalyst was regenerated after the reaction through impregnation with 2-octanol and DA at 250 °C. After the regeneration process, the catalyst could be reused for four runs.

In the distribution test, it could be observed that the hydrophobic DA-CoO remained in a highly distributed state in the organic phase (Fig. S14), while the commercial hydrophilic CoO nanoparticle was distributed in the water phase. This experiment was in accordance with the WCA test, confirming the high affinity towards the organic molecule and the strong water repellent ability. This property could hinder the inevitable adsorption of water on the active site, and uniform dispersal during the reaction could be achieved, as was the case in our previous report. Accordingly, excellent catalytic performance was achieved with the hydrophobic catalyst.

The hydrophobic DA-CoO catalyst was not only active for ethylbenzene oxidation, but also for the selective oxidation of tetralin and mesitylene (Table 2). The hydrophobic and hydrophilic DA-CoO catalyst exhibited similar effects under the

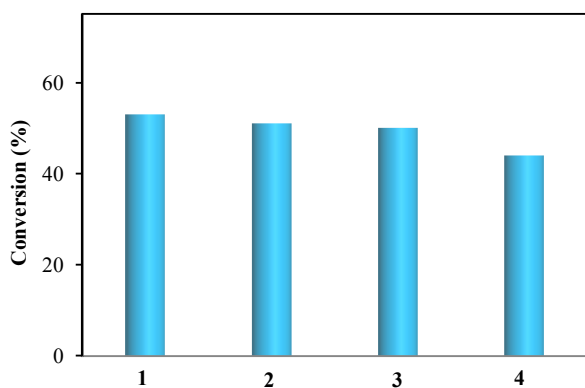


Fig. 6. Cycle tests on DA-CoO. Reaction conditions: ethylbenzene (80 mmol), catalyst (20 mg), 1.0 MPa O₂, TBHP (80 mg) as initiator, 120 °C, and 8 h.

Table 2

Comparative selective oxidation of tetralin and mesitylene using different catalysts.

Entry	Catalyst	Conversion (%)	Distribution of products (%)				Mass-specific activity (mmol g _{cat} ⁻¹ h ⁻¹)
			2b	2c	Others		
1	CoO	32	37	57	6	256	
2	DA-CoO	63	32	56	12	503	

Entry	Catalyst	Conversion (%)	Distribution of products (%)				Mass-specific activity (mmol g _{cat} ⁻¹ h ⁻¹)
			3b	3c	3d	Others	
1	CoO	25	34	35	29	2	306
2	DA-CoO	52	15	17	55	13	637

Reaction conditions: catalyst (20 mg), reactant (74 mmol), TBHP as initiator (80 mg), O₂ as oxidant.

same conditions; the conversion of tetralin and mesitylene increased from 32% to 63% and 25% to 52%, respectively. In addition, the selectivity of deep oxidation products also increased, in accordance with the ethylbenzene oxidation.

In summary, through surface modification, a new hydrophobic CoO nanoparticle coating by amines was synthesized, which showed high activity towards the selective oxidation of aromatic hydrocarbons. The surface-amines coated CoO nanoparticles exhibited hydrophobic properties, with a WCA of 143°. It is believed that the hydrophobic property of the CoO surface is an important factor for high catalytic performance.

References

- [1] A. K. Suresh, M. M. Sharma, T. Sridhar, *Ind. Eng. Chem. Res.*, **2000**, 39, 3958–3997.
- [2] J. M. Thomas, R. Raja, G. Sankar, R. G. Bell, *Nature*, **1999**, 398, 227–230.
- [3] T. Punniyamurthy, S. Velusamy, J. Iqbal, *Chem. Rev.*, **2005**, 105, 2329–2363.
- [4] M. S. Hamdy, A. Ramanathan, T. Maschmeyer, U. Hanefeld, J. C. Jansen, *Chem. -Eur. J.*, **2006**, 12, 1782–1789.
- [5] C. Chen, J. Xu, Q. Zhang, Y. Ma, L. Zhou, M. Wang, *Chem. Commun.*, **2011**, 47, 1336–1338.
- [6] X. Li, L. Zhou, J. Gao, H. Miao, H. Zhang, J. Xu, *Powder Technol.*, **2009**, 190, 324–326.
- [7] G. Zhang, D. E. Wang, P. Feng, S. Shi, C. Wang, A. Zheng, G. Lü, Z. Tian, *Chin. J. Catal.*, **2017**, 38, 1207–1215.
- [8] M. Y. Zhang, L. F. Wang, H. B. Ji, B. Wu, X. P. Zeng, *J. Nat. Gas Chem.*, **2007**, 16, 393–398.
- [9] C. Zhang, Y. Bai, Y. Yin, J. Gu, Y. Sun, *Korean J. Chem. Eng.*, **2011**, 28, 602–607.
- [10] D. N. Srivastava, N. Perkas, G. A. Seisenbaeva, Y. Kolytyn, V. G. Kessler, A. Gedanken, *Ultrason. Sonochem.*, **2003**, 10, 1–9.
- [11] L. Zhou, J. Xu, H. Miao, F. Wang, X. Li, *Appl. Catal. A*, **2005**, 292, 223–228.

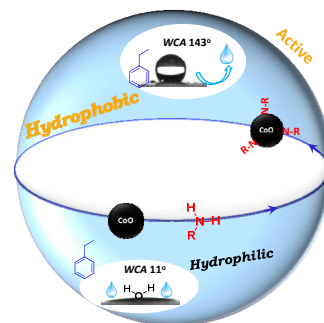
Graphical Abstract

Chin. J. Catal., 2019, 40: 1488–1493 doi: S1872-2067(19)63413-3

Aliphatic amines modified CoO nanoparticles for catalytic oxidation of aromatic hydrocarbon with molecular oxygen

Meng Liu, Song Shi*, Li Zhao, Chen Chen, Jin Gao, Jie Xu*
Dalian Institute of Chemical Physics, Chinese Academy of Sciences;
University of Chinese Academy of Sciences; Ningbo University

The amines-modified CoO nanoparticles exhibited hydrophobic properties with a water contact angle of 143°, which was accompanied by better performance in the hydrocarbon oxidation process compared to that of the hydrophilic commercial CoO nanoparticles.



- [12] T. Liu, H. Cheng, L. Sun, F. Liang, C. Zhang, Z. Ying, W. Lin, F. Zhao, *Appl. Catal. A*, **2016**, 512, 9–14.
- [13] H. Li, L. Li, Y. Li, *Nanotechnol. Rev.*, **2013**, 2, 515–518.
- [14] W. Shi, L. Cao, H. Zhang, X. Zhou, B. An, Z. Lin, R. Dai, J. Li, C. Wang, W. Lin, *Angew. Chem. Int. Ed.*, **2017**, 56, 9704–9709.
- [15] C. Chen, J. Xu, Q. Zhang, H. Ma, H. Miao, L. Zhou, *J. Phys. Chem. C*, **2009**, 113, 2855–2860.
- [16] M. Wang, C. Chen, Q. Zhang, Z. Du, Z. Zhang, J. Gao, J. Xu, *J. Chem. Technol. Biotechnol.*, **2010**, 85, 283–287.
- [17] C. Chen, S. Shi, M. Wang, H. Ma, L. Zhou, J. Xu, *J. Mater. Chem. A*, **2014**, 2, 8126–8134.
- [18] L. Wang, F.-S. Xiao, *ChemCatChem*, **2014**, 6, 3048–3052.
- [19] T. Li, J. Wang, F. Wang, L. Zhang, Y. Jiang, H. Arandiyan, H. Li, *ChemCatChem*, **2019**, 11, 1576–1586.
- [20] J. Zhang, X. Liu, R. Blume, A. Zhang, R. Schlögl, D. S. Su, *Science*, **2008**, 322, 73–77.
- [21] F. Studt, F. Abild-Pedersen, T. Bligaard, R. Z. Sorensen, C. H. Christensen, J. K. Norskov, *Angew. Chem. Int. Ed.*, **2008**, 47, 9299–9302.
- [22] L. D. Ellis, R. M. Trotter, C. B. Musgrave, D. K. Schwartz, J. W. Medlin, *ACS Catal.*, **2017**, 7, 8351–8357.
- [23] X. Jia, J. Ma, F. Xia, Y. Xu, J. Gao, J. Xu, *Nat. Commun.*, **2018**, 9, 933.
- [24] M. Tamura, R. Kishi, Y. Nakagawa, K. Tomishige, *Nat. Commun.*, **2015**, 6, 8580.
- [25] L. Li, X. Sun, X. Qiu, J. Xu, G. Li, *Inorg. Chem.*, **2008**, 47, 8839–8846.
- [26] X. Liu, M. Atwater, J. Wang, Q. Dai, J. Zou, J. P. Brennan, Q. Huo, *J. Nanosci. Nanotechnol.*, **2007**, 7, 3126–3133.
- [27] Y. Tian, B. Yu, X. Li, K. Li, *J. Mater. Chem.*, **2011**, 21, 2476–2481.
- [28] Z. Xu, C. Shen, Y. Hou, H. Gao, S. Sun, *Chem. Mater.*, **2009**, 21, 1778–1780.
- [29] B. Ernst, S. Libs, P. Chaumette, A. Kiennemann, *Appl. Catal. A*, **1999**, 186, 145–168.
- [30] T. Garcia, S. Agouram, J. F. Sánchez-Royo, R. Murillo, A. M. Mastral, A. Aranda, I. Vázquez, A. Dejoz, B. Solsona, *Appl. Catal. A*, **2010**, 386, 16–27.
- [31] Y. Chen, S. Zhao, Z. Liu, *Phys. Chem. Chem. Phys.*, **2015**, 17, 14012–14020.
- [32] K. B. Klepper, O. Nilsen, H. Fjellvåg, *Thin Solid Films*, **2007**, 515, 7772–7781.

脂肪胺修饰的CoO纳米粒子催化分子氧选择氧化芳香烃

刘梦^{a,b}, 石松^{a,#}, 赵丽^{a,b}, 陈晨^{a,c}, 高进^a, 徐杰^{a,*}

^a中国科学院大连化学物理研究所催化基础国家重点实验室, 洁净能源国家实验室(筹), 辽宁大连116023

^b中国科学院大学, 北京 100049

^c宁波大学材料科学与化学工程学院, 浙江宁波 315211

摘要: 以分子氧为氧化剂实现烃类的选择氧化在学术研究和工业应用中均具有重要的意义. 钴氧化物(CoO_x)纳米粒子在催化烃类选择氧化过程中具有较高的催化活性, 其粒径、孔结构以及组分等因素均对催化活性有着重要的影响. 由于烃类氧化反应过程中生成的产物分子极性大于底物分子, 使得疏水的催化剂对该类反应有利. 而 CoO_x 由于自身表面羟基的存在呈亲水性, 因此可以通过疏水修饰进一步提升 CoO_x 的催化活性. 我们课题组报道了通过有机硅烷的修饰方法制备了疏水钴基二氧化硅材料, 该过程是通过对接体的间接修饰而达到调控催化剂亲疏水微环境的目的. 然而, 关于 CoO_x 活性位点的直接疏水修饰较少报道, 对于 CoO_x 进行修饰制备疏水纳米粒子是一个具有挑战性的工作.

本文利用有机胺对 CoO_x 纳米粒子进行有机修饰, 得到了丁胺(BA)修饰的BA- CoO 和十二胺(DA)修饰的DA- CoO 催化剂, 静态水滴接触角分别为 126° 和 143° , 证明了其表面呈疏水性, 并且二者疏水角度具有一定的差异. 通过X射线粉末衍

射测定了催化剂的晶型为立方相CoO, 从高分辨透射电镜结果也观察到了CoO(111)晶面的晶格条纹, 晶面间距为0.25 nm. 通过透射电镜表征方法, 对纳米粒子的形貌和粒径大小进行分析, BA-CoO和DA-CoO均为纳米立方体的形貌, 其中DA-CoO的纳米粒子相对均匀并且粒径更小, 这可能是由于DA的碱性相对于BA较弱, 从而使得前驱体分解更慢导致. 进一步通过红外光谱和X射线光电子能谱证明了纳米粒子中有有机胺的存在.

在催化芳香烃类分子氧氧化反应中, 疏水性的DA-CoO和BA-CoO均表现出比亲水性的CoO更高的催化活性, 其中DA-CoO催化乙苯转化率为53%, 苯乙酮选择性为78%; 而亲水的CoO对应的转化率和选择性分别为18%和69%. 通过利用DA和2-辛醇体系对商品化的CoO进行修饰, 经过250 °C处理5 h得到了疏水的CoO, 水滴接触角为143°. 将该催化剂应用在乙苯氧化中, 对比处理前后的催化剂活性, 转化率从18%提高到45%, 这说明疏水性质是影响CoO催化乙苯氧化活性的重要因素. 有机胺修饰的CoO纳米粒子在烃类催化氧化中的活性增加, 这种有机胺修饰的方法为其它金属氧化物的疏水性修饰提供了参考.

关键词: 烃氧化; 疏水修饰; 有机胺修饰; 钴氧化物; 表面修饰

收稿日期: 2019-06-28. 接受日期: 2019-07-19. 出版日期: 2019-10-05.

*通讯联系人. 电话/传真: (0411)84379245; 电子信箱: xujie@dicp.ac.cn

#通讯联系人. 电话/传真: (0411)84379277; 电子信箱: shisong@dicp.ac.cn

基金来源: 国家自然科学基金(21790331, 21603218); 中国科学院战略性先导科技专项(XDA21030400, XDB17020300).

本文的电子版全文由Elsevier出版社在ScienceDirect上出版(<http://www.sciencedirect.com/science/journal/18722067>).